Available online at www.sciencedirect.com
ScienceDirect
Ore Geology Reviews 33 (2008) 117–133
ORE GEOLOGY REVIEWS
www.elsevier.com/locate/oregeorev

Stable isotope geochemistry of carbonate minerals in supergene oxidation zones of Zn–Pb deposits

H. Albert Gilg [a,*], Maria Boni [b,c], Rupert Hochleitner [d], Ulrich Struck [e,1]

[a] Lehrstuhl für Ingenieurgeologie, Technische Universität München, Arcisstr. 21, 80333 München, Germany
[b] Dipartimento di Scienze della Terra, Università di Napoli "Federico II", 80134 Napoli, Italy
[c] Geologisch-Palaeontologisches Institut, Universität Heidelberg, 69120 Heidelberg, Germany
[d] Mineralogische Staatssammlung München, München, 80333 München, Germany
[e] GeoBioCentre^{LMU}, Ludwig-Maximilians-Universität München, 80333 München, Germany

Received 28 November 2006; accepted 7 February 2007
Available online 1 August 2007

Abstract

The $^{18}O/^{16}O$ and $^{13}C/^{12}C$ ratios of carbonate minerals formed by supergene oxidation of Zn–Pb deposits and submarine alteration of ancient slags were studied in order to constrain isotope fractionation factors for smithsonite, cerussite, and phosgenite, and to characterize conditions of nonsulfide ore formation. We present new isotope data of carbonate-hosted ores from the Iglesiente district (Sardinia, Italy) and Vila Ruiva (Portugal), as well as from the silicate-hosted ores of the Broken Hill district, New South Wales (Australia) and Freihung (Germany) and review previously published isotope data. The temperature dependence of oxygen isotope fractionation between Pb and Zn carbonate minerals and water below 240 °C for cerussite and below 100 °C for smithsonite and phosgenite can be expressed as

$$1000\ln\alpha_{\text{cerussite–water}} = 2.29(10^6/T^2)-3.56$$

$$1000\ln\alpha_{\text{smithsonite–water}} = 3.10(10^6/T^2)-3.50$$

$$1000\ln\alpha_{\text{phosgenite–water}} = 2.55(10^6/T^2)-3.50$$

with T in Kelvin. The carbon isotope fractionation between smithsonite, phosgenite, hydrozincite and calcite is less than about 2‰, while cerussites are strongly depleted in ^{13}C by about 10‰ as compared to the former minerals. Oxygen isotope variations of individual carbonate minerals within a deposit are relatively small indicating constant formation temperatures and a single, meteoric fluid source. Average formation temperatures of the studied deposits are calculated at 20±5 °C using the estimated isotope compositions of local paleometeoric waters. We observe a linear relationship between the isotope values of estimated paleometeoric waters and supergene carbonates. Thus, base metal carbonate minerals from supergene deposits may provide paleoclimatic information. The carbon isotope values are in most carbonate-hosted deposits highly variable (more than 10‰) suggesting at least two isotopically distinct carbon sources. The isotopically light component can be related to oxidation of C3 plants (soil-derived carbon) and/or microbes that take active part in sulfide oxidation, while the isotopically heavy component

* Corresponding author. Tel.: +49 89 289 25855; fax: +49 89 289 25852.
E-mail address: agilg@tum.de (H.A. Gilg).
[1] Present address: Museum für Naturkunde, Humboldt-Universität Berlin, 10099 Berlin, Germany.

doi:10.1016/j.oregeorev.2007.02.005

originates from carbonate carbon from wall rocks and/or atmospheric carbon. The ^{13}C-enriched component is less dominant in silicate-hosted deposits.

Keywords: Oxygen isotopes; Carbon isotopes; Smithsonite; Cerussite; Phosgenite; Nonsulfide Zn–Pb deposits

1. Introduction

Stable oxygen and carbon isotope data of carbonate minerals associated to hydrothermal, diagenetic, and magmatic sulfide ore deposits have for many years yielded valuable information on the temperatures of mineralization, origins and evolution of ore-forming fluids, mechanisms of ore deposition, and patterns of wall-rock alteration (e.g., Ohmoto and Rye, 1979; Field and Fifarek, 1985; Zheng and Hoefs, 1993; Schwinn et al., 2006). In contrast, comparably few isotope studies have been published on carbonates from sulfide oxidation zones or hypogene nonsulfide Zn–Pb deposits (e.g., Wickman et al., 1951; Monteiro et al., 1999; Melchiorre et al., 1999, 2000, 2001; Melchiorre and Williams, 2001; Boni et al., 2003a; Gilg and Boni, 2004). In the light of recent developments of nonsulfide zinc deposits (e.g., Hitzman et al., 2003), such isotope studies might be very important to distinguish supergene from hypogene base metal carbonate deposits, to evaluate the effects of oxidative heating and the role of microbes during sulfide oxidation. Additionally, the isotope data may help to determine the type of fluid (meteoric or sea water) involved in sulfide oxidation, to trace changes of isotope compositions of meteoric waters and thus to gain indirect information on the duration of sulfide oxidation, to distinguish sulfide versus carbonate wall rock replacement ("exotic") deposits, and to trace metal enrichments versus dilution processes. Additionally, even paleoclimatic information might be gained from such analyses.

Sulfur isotope ratios of sulfates from sulfide oxidation zones (e.g., Gavelin et al., 1960; Field, 1966), as well as $\delta^{66}Zn$ values from supergene Zn carbonates (Maréchal et al., 1999), generally show no significant fractionation with respect to the precursor sulfide minerals and are thus in contrast to C–O-isotopes of carbonate minerals, less helpful in understanding sulfide oxidation processes. However, bacterial sulfate reduction in oxidation zone may significantly fractionate sulfur and oxygen isotope compositions in the residual sulfate (e.g., Seal, 2003) and lead to extreme ^{34}S depletions in newly formed supergene sulfides (e.g., Bawden et al., 2003).

In this study, we review oxygen and carbon isotope fractionation effects on Zn, Pb and associated Ca carbonate minerals derived from theoretical and experimental studies and the previously published isotope values for such minerals. Additionally, we will present a new set of isotope data from a variety of nonsulfide Zn–Pb deposits (Iglesiente district — Sardinia, Broken Hill — New South Wales, Vila Ruiva — Portugal, Freihung — Bavaria) and from slag minerals formed in a submarine environment at Lavrion, Greece. These empirical data will be used to derive new oxygen isotope fractionation equations for Zn and Pb carbonate minerals and water. Additionally, we will discuss implications of stable isotope geochemical studies in supergene settings for ore genesis and paleoclimate.

2. Fractionation factors

2.1. Oxygen

A prerequisite for the interpretation of stable isotope data is the accurate determination of the isotope compositions and the knowledge of fractionation factors between minerals and fluids as a function of temperature. The oxygen isotope fractionation between CO_2 liberated from the mineral during reaction with phosphoric acid and carbonate ($\alpha^{phos}{}_{CO_2-carbonate}$) has to be considered in this respect. The acid fractionation factors have recently been determined for smithsonite and cerussite between 25 and 72 °C and were shown to be different from the values for calcite (Gilg et al., 2003b):

$$1000\ln\alpha^{phos}{}_{CO_2-smithsonite} = 3.96 + 6.69\ 10^5/T^2 \quad (1)$$

$$1000\ln\alpha^{phos}{}_{CO_2-cerussite} = 5.13 + 4.79\ 10^5/T^2 \quad (2)$$

$$1000\ln\alpha^{phos}{}_{CO_2-calcite} = 3.95 + 5.53\ 10^5/T^2 \quad (3)$$

with T in Kelvin.

The acid fractionation factors for phosgenite [$Pb_2Cl_2CO_3$] and hydrozincite [$Zn_5(OH)_6(CO_3)_2$] have not yet been determined. We use here the values of cerussite for phosgenite and of calcite for fast-reacting aragonite and hydrozincite (O'Neil, 1986).

The oxygen isotope fractionations between base metal carbonates and water, as well as their variations with temperature, are still poorly constrained. Three different approaches have generally been pursued: theoretical calculations, experiments, and empirical observations. The results of theoretical and semi-empirical determination of oxygen isotope fractionations between carbonate and water for smithsonite, cerussite and calcite are shown in Fig. 1. Golyshev et al. (1981) calculated the reduced partition functions for a variety of carbonate minerals including smithsonite, cerussite, and calcite. At 300 K (~27 °C) and equilibrium conditions, smithsonite is predicted to be 2.5‰ heavier and cerussite 9.5‰ lighter than calcite. Similar relative results have been obtained by Zheng (1999) using the modified increment method. According to his equations, smithsonite should be 2.8 to 3.9‰ heavier and cerussite about 5.4 to 6.7‰ lighter than calcite in the temperature range between 5 and 50 °C. The absolute values for oxygen isotope fractionation between carbonate and water are, however, not consistent (Fig. 1). We note that both approaches use several assumptions and corrections that significantly influence the results. O'Neil et al. (1969) determined an oxygen isotope fractionation between calcite and cerussite of 3.2‰ at 240 °C using statistical–mechanical calculations. No calculations for low temperatures were presented. However, based on their calculations for Sr and Ba carbonates at various temperatures, an increase of the calcite–cerussite fractionation at lower temperatures probably in the order of several ‰ can be expected.

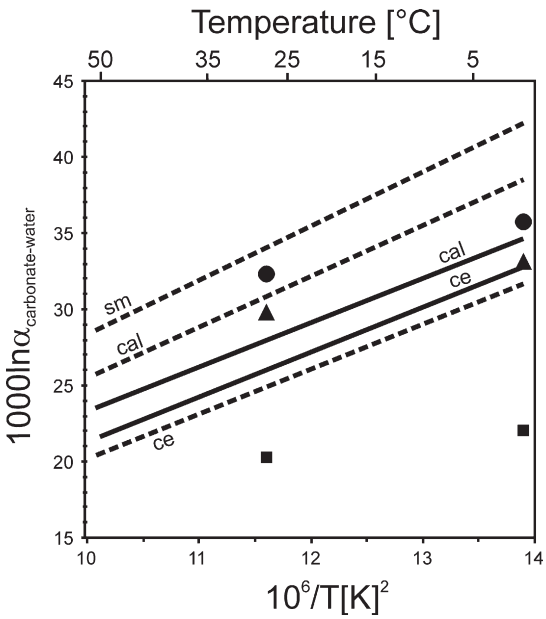

Fig. 1. Theoretical and experimental oxygen isotope fractionation for carbonate–water systems: smithsonite (sm, circles), calcite (cal, triangles) and cerussite (ce, squares). Dotted lines from Zheng (1999), individual symbols from Golyshev et al. (1981), solid lines from O'Neil et al. (1969) for calcite and Melchiorre et al. (2001) for cerussite.

Experimental calibrations of isotope equilibrium between two phases ideally involve exchange reactions. Such experiments have been carried out by O'Neil et al. (1969) for the systems calcite–water and cerussite–water at temperatures of 240 and 210 °C. The $1000\ln\alpha_{\text{cerussite–water}}$ is 4.5‰ at 240 °C and thus 2.7‰ smaller than the experimental value for calcite–water. At 210 °C the $1000\ln\alpha_{\text{cerussite–water}}$ is 6.9‰ and thus 2.5‰ smaller than the value for calcite–water.

At low temperatures (<200 °C), however, isotope exchange reactions between carbonates and water are too slow to reach equilibrium. Therefore, synthesis reactions using a slow precipitation method have been applied for calcite and few other carbonates and gave results that were generally consistent with most empirical and theoretical determinations (e.g., McCrea, 1950; O'Neil et al., 1969; Kim and O'Neil, 1997). The most commonly used oxygen isotope fractionation equation for calcite (O'Neil et al., 1969; Friedman and O'Neil, 1977) is:

$$1000\ln\alpha_{\text{calcite–water}} = 2.78(10^6/T^2) - 2.89 \quad (4)$$

with T in Kelvin.

Melchiorre et al. (2001) used a modified synthesis approach to derive an oxygen isotope fractionation equation for cerussite–water. Cerussite was crystallized by reaction of a lead nitrate solution with calcite cleavage fragments in the temperature range of 20 to 65 °C. Melchiorre et al. (2001) used the phosphoric acid fractionation factor of calcite (1.01024) for cerussite to derive their fractionation equation. We have recalculated here their experimental data using the new cerussite acid fractionation factor of 1.01061 at 25°C (Gilg et al., 2003b):

$$1000\ln\alpha_{\text{cerussite–water}} = 2.65(10^6/T^2) - 4.20 \quad (5)$$

with T in Kelvin. These two experimental equations (Fig. 1) predict that in an equilibrium situation, cerussite is isotopically 2.6 to 3.1‰ lighter than calcite at temperatures between 50 and 0 °C. These differences are much smaller than the predictions derived from the theoretical equations.

Empirical calibrations of the oxygen isotope fractionation factors are rare for base metal carbonates. Melchiorre

Table 1
C and O isotope data of Zn, Pb and Ca carbonates from supergene deposits

Sample no	Mineral	Description	Location	$\delta^{13}C_{VPDB}$	$\delta^{18}O_{VSMOW}$	Reference
Iglesiente District, SW Sardinia, Italy						
27-G	sm	Rounded leached crystals	Seddas Moddizzis	−6.8	27.5	Boni et al. (2003a)
20-Ga	sm	Massive	Seddas Moddizzis	−5.7	26.2	Boni et al. (2003a)
20-G	sm	Rose concretion	Seddas Moddizzis	−3.9	25.7	Boni et al. (2003a)
25-G	sm	Yellow concretion	Nebida Can.San Giuseppe	−2.0	26.5	Boni et al. (2003a)
24-G	sm	Botryoidal concretion	Nebida Can.San Giuseppe	−1.8	26.5	Boni et al. (2003a)
25-Ga	sm	Massive	Nebida Can.San Giuseppe	−4.9	27.3	Boni et al. (2003a)
12-G	sm	Clear rhombohedral crystals	Nebida level +92	−10.4	26.1	Boni et al. (2003a)
13-G	sm	Dark rhombohedral crystals	Nebida level +92	−10.1	27.4	Boni et al. (2003a)
13-Ga	sm	Massive	Nebida level +92	−9.3	28.8	Boni et al. (2003a)
48-Ga	sm	Massive	Nebida level +92	−8.8	28.0	Boni et al. (2003a)
49-G	sm	Massive	Nebida level +92	−7.7	28.8	Boni et al. (2003a)
50-G	sm	Clayey massive	Nebida level +92	−7.3	28.7	Boni et al. (2003a)
29-Ga	sm	Massive	Mount Agruxiau	−4.0	28.5	Boni et al. (2003a)
8-G	sm	Yellow “rice grain” crystals	Mount Agruxiau	−6.4	28.0	Boni et al. (2003a)
9-G	sm	White “rice grain” crystals	Mount Agruxiau	−6.9	26.5	Boni et al. (2003a)
65-G	sm	Pseudomorph after calcite	Campo Pisano	−6.2	28.8	Boni et al. (2003a)
Sar1a	sm	White powdery coating sample Sar1	Masua-Lanusei	−7.1	27.5	Boni et al. (2003a)
Sar1b	sm	Orange crust coating sample Sar1	Masua-Lanusei	−7.9	28.9	Boni et al. (2003a)
Sar1	sm	Yellow stalactite (Cd)	Masua-Lanusei	−2.4	28.8	Boni et al. (2003a)
18-G	sm	Crust (platy crystals)	San Giovanni	−8.2	27.4	Boni et al. (2003a)
52-G	sm	White stalactite	San Giovanni	−2.0	28.0	Boni et al. (2003a)
36-G	sm	Concretion (platy crystals)	San Benedetto	−8.0	27.9	Boni et al. (2003a)
63-G	sm	Concretion (platy crystals)	Monteponi-Cungiaus	−5.8	27.4	Boni et al. (2003a)
64-G	sm	Small white concretion	Monteponi-Cungiaus	−0.6	27.5	Boni et al. (2003a)
Sar2b	sm	Grey concretion	Monteponi	−3.2	28.5	Boni et al. (2003a)
Sar-3	hz	White powder	San Giovanni	−7.1	27.0	Boni et al. (2003a)
45-G	hz	Botryoidal crust	Monteponi	−2.4	26.6	Boni et al. (2003a)
10-G	ce	Clear crystals	Monteponi	−11.6	17.1	Boni et al. (2003a)
TUM-Ce-1	ce	Clear crystal	Monteponi	−21.0	16.8	This study
SPE-26	ce	Clear crystals with galena	Monteponi	−10.0	16.7	This study
SPE-26b	ce	Clear crystals with galena	Monteponi	−10.2	16.7	This study
SPE-28	ce	White crystals with goethite	Tiny–Arenas	−18.3	17.8	This study
MSM 52509	ce	White twinned crystal on galena	Monteponi	−11.3	17.8	This study
MSM 52511	ce	Prismatic grey crystal on galena	Monteponi	−14.6	17.6	This study
MSM 52514	ce	Clear twin crystals with goethite	Monteponi	−6.5	17.2	This study
HAM-1	ce	Acicular crystals on goethite	Monteponi	−18.1	17.8	This study
MPB-1	ce	White fibrous crystals	Monteponi	−16.5	18.0	This study
MP-1	pg	Clear crystals	Monteponi	−7.2	21.1	Boni et al. (2003a)
MP-3	pg	Clear crystals	Monteponi	−9.2	20.7	Boni et al. (2003a)
MSM 28908	pg	Prismatic brownish crystals on galena	Monteponi	−6.7	20.4	This study
MSM 52630	pg	Clear to brownish crystals on galena	Monteponi	−5.9	20.1	This study
MSM 52636	pg	Clear crystals on galena with cerussite	Monteponi	−9.8	20.4	This study
MSM 52634	pg	Thick tabular crystals on galena	Monteponi	−4.2	21.2	This study
33-G	cc	Concretion	Nebida-Carroccia	−9.2	24.7	Boni et al. (2003a)
38-G	cc	Crystals	Monteponi-Nicolay	−9.8	25.6	Boni et al. (2003a)
40-G	cc	Crystals	Monteponi-Villamarina	−10.1	24.8	Boni et al. (2003a)
41-G	cc	Crystals	Monteponi-Villamarina	−10.2	24.8	Boni et al. (2003a)
62-G	cc	Crystals	Buggerru	−11.3	25.4	Boni et al. (2003a)
Liège district, Eastern Belgium						
RN1996a	sm	Clear crystals, outer part	Moresnet	−9.8	28.8	Coppola et al. (2007-this volume)
RN1996b	sm	Yellowish crust, inner part	Moresnet	−11.6	28.2	Coppola et al. (2007-this volume)

Table 1 (*continued*)

Sample no	Mineral	Description	Location	$\delta^{13}C_{VPDB}$	$\delta^{18}O_{VSMOW}$	Reference
Liège district, Eastern Belgium						
RN2008c	sm	Brownish massive matrix of breccia	Moresnet	−8.8	28.1	Coppola et al. (2007-this volume)
RN2101c	sm	Late clear crystals	Moresnet	−10.9	28.1	Coppola et al. (2007-this volume)
RN2008b	sm	Yellow crystals on RN2008c	Moresnet	−8.6	28.1	Coppola et al. (2007-this volume)
RN4106	sm	Reddish brown banded sediment	Moresnet	−7.4	30.6	Coppola et al. (2007-this volume)
RN2017	sm	White crystals	La Calamine	−10.7	28.3	Coppola et al. (2007-this volume)
RN2044c	sm	Yellowish crystals	La Calamine	−1.5	28.1	Coppola et al. (2007-this volume)
RN2051a	sm	Brownish matrix of mottled breccia	La Calamine	−9.8	28.7	Coppola et al. (2007-this volume)
RA4999a	sm	Greyish central part of concretion	La Calamine	−6.2	28.0	Coppola et al. (2007-this volume)
RA4999b	sm	Yellowish porous outer part of concretion	La Calamine	−6.6	27.4	Coppola et al. (2007-this volume)
R2B35/3925	sm	Brownish massive	La Calamine	−9.2	28.4	Coppola et al. (2007-this volume)
RN2208a	sm	Yellowish clear crystals, outer part	Fossey	−11.6	28.3	Coppola et al. (2007-this volume)
RN2300d	sm	Clear crystals	Fossey	−10.2	28.6	Coppola et al. (2007-this volume)
RN2208c	sm	Fe-rich, Brownish massive matrix	Fossey	−7.6	30.2	Coppola et al. (2007-this volume)
RN2220a	sm	Black sulfide-bearing crystals, inner part	Welkenraedt	−10.1	28.9	Coppola et al. (2007-this volume)
RN2220b	sm	Yellowish clear crystals, outer part	Welkenraedt	−10.2	28.2	Coppola et al. (2007-this volume)
RN2224b	sm	brown crystals	Welkenraedt	−8.4	29.5	Coppola et al. (2007-this volume)
RN2236a	sm	Globular greyish concretion, outer part	Welkenraedt	−7.1	27.2	Coppola et al. (2007-this volume)
RN2236b	sm	Brownish massive inner part	Welkenraedt	−3.2	27.1	Coppola et al. (2007-this volume)
RA4986a	sm	White botryoidal concretion	Welkenraedt	−8.9	28.2	Coppola et al. (2007-this volume)
RN2270a	sm	White concretion, outer part	Theux	−2.2	27.7	Coppola et al. (2007-this volume)
RN2270b	sm	Brownish, massive inner part	Theux	−1.6	28.1	Coppola et al. (2007-this volume)
RA 7898	ce	Fibrous crystals	Theux	−14.7	17.6	Coppola et al. (2007-this volume)
RA 8497	ce	Clear crystals	Theux	−15.0	17.2	Coppola et al. (2007-this volume)
RN 2330	ce	White fibrous crystals	Theux	−14.8	16.8	Coppola et al. (2007-this volume)
RA 8494	ce	Fibrous crystals	Angleur	−15.1	18.4	Coppola et al. (2007-this volume)
RN 2339	ce	Greyish massive aggregate	Welkenraedt	−18.4	19.3	Coppola et al. (2007-this volume)
RN2487b	cc	Green botryoidal crust	Moresnet	−10.4	24.7	Coppola et al. (2007-this volume)
Be4a	cc	White vitreous crystals	La Calamine	−7.4	25.7	Coppola et al. (2007-this volume)
Be5b	cc	Red vitreous crystals	La Calamine	−6.5	25.5	Coppola et al. (2007-this volume)
Be8c	cc	Red vitreous crystals	La Calamine	−6.5	25.7	Coppola et al. (2007-this volume)
Be9b	cc	Red vitreous crystals	La Calamine	−6.1	25.5	Coppola et al. (2007-this volume)
Broken Hill, New South Wales, Australia						
M41949-1	sm	Mn-rich (21 mol% MnCO3)	Broken Hill	−12.0	27.6	Böttcher et al. (1993)
MSM 7881A	sm	Clear botryoidal crust, inner part	Broken Hill	−7.8	27.5	This study
MSM 7881B	sm	Clear botryoidal crust, outer part	Broken Hill	−8.8	28.2	This study
SAM G11959a	sm	Clear botryoidal crust on Mn-oxide	Broken Hill	−8.9	27.4	This study
SAM G2184	sm	Clear scalenohedra on goethite	Broken Hill	−8.0	26.4	This study
SAM 20435	sm	Clear crystal	Broken Hill	−8.7	28.7 27.631893	This study
K2259	ce	–	Block-4, 1703N, 228W	and 14.9	16.6	Melchiorre et al. (2001)
K2266	ce	–	Block-4, 1760N, 172W	−19.2	16.9	Melchiorre et al. (2001)
K2265	ce	–	Block-4, 1855N, 160W	−18.9	16.6	Melchiorre et al. (2001)
K2264	ce	–	Block-4, 1990N, 175W	−14.6	16.3	Melchiorre et al. (2001)
A-BH15	ce	–	“first level”	−17.2	15.6	Melchiorre et al. (2001)
A-BH16	ce	–	“first level”	−16.9	15.7	Melchiorre et al. (2001)
A-BH17	ce	–	“first level”	−18.3	15.4	Melchiorre et al. (2001)
K2263	ce	–	Kintore open pit, 1357N, 181W	−15.7	16.2	Melchiorre et al. (2001)

(continued on next page)

Table 1 (*continued*)

Sample no	Mineral	Description	Location	$\delta^{13}C_{VPDB}$	$\delta^{18}O_{VSMOW}$	Reference
Broken Hill, New South Wales, Australia						
K2260	ce	–	Kintore open pit, 360N, 180W	−13.9	16.4	Melchiorre et al. (2001)
K2258	ce	–	Kintore open pit, 390N, 200W	−13.5	15.8	Melchiorre et al. (2001)
Alto Alentejo District, Portugal						
Pre-1	sm	White crystal	Vila Ruiva	−10.8	30.6	This study
Prg-9S	sm	White, fine, crystals	Vila Ruiva	−10.5	29.6	This study
Prg 12S	sm	White	Vila Ruiva	−11.0	29.7	This study
Prg-17S	sm	White, crystals, small	Vila Ruiva	and 10.7	30.0	This study
Prg-18S	sm		Vila Ruiva	−10.5	29.7	This study
Prg-8	cc	Clear crystals on goethite	Vila Ruiva	−11.0	30.6	This study
Skorpion, Namibia						
BH 7007	sm		Siliciclastic unit	−6.0	27.7	Borg et al. (2003)
0807	sm		Siliciclastic unit	−4.0	27.8	Borg et al. (2003)
8027	sm		Siliciclastic unit	−8.0	28.3	Borg et al. (2003)
0727	sm		Siliciclastic unit	−6.9	27.8	Borg et al. (2003)
O711	sm		Siliciclastic unit	−6.9	27.5	Borg et al. (2003)
Tui, New Zealand				1.5	0.3	
R3479/4	sm	Brown	Ruakaka, No. 3 level	−5.8	28.0	Robinson (1974)
R3479/10	sm	Blocky	Ruakaka, No. 4 level, Raise 9	−6.5	28.1	Robinson (1974)
R3479/12	ce	Late vug filling	Ruakaka, No 2 level	−16.5	19.7	Robinson (1974)
Triades, Greece						
	ce		Triades	−18.5	18.7	Liakopoulos (1987)
Garpenberg, Sweden						
	ce	Earthy ore		−21.2	11.6	Vivallo and Broman (1993)
Freihung, Germany						
Fr 1	ce	White crystals in vein		−20.0	15.2	This study
Fr 4	ce	White crystals in vein		−13.8	15.7	This study
Fr 4	ce			−14.1	15.4	This study
Fr 5	ce	White cement of sandstone		−15.8	14.7	This study
Fr 5	ce			−15.8	15.0	This study
Fr 6	ce	Yellow-green crystals in vein		−20.2	14.6	This study

et al. (2001) reported on cerussites formed on timber in abandoned mines (Bwlch Glas mine, Wales, U.K., and Pinnacles Mine, New South Wales, Australia). They measured temperature and isotope composition of mine waters and cerussite. The recalculated fractionation factors ($1000\ln\alpha_{cerussite-water}$) using the phosphoric acid fractionation factors of Gilg et al. (2003b) are 25.98‰ at 10.2 °C for the Bwlch Glas, and 25.64‰ at 23 °C for the Pinnacles sample. Both values plot 2.83‰ (Bwlch Glas mine) to 0.38‰ (Pinnacles) below the predictions of Eq. (5).

2.2. Carbon

Theoretical statistical–mechanical calculations on $^{13}C/^{12}C$ fractionation between various carbonates were presented by Golyshev et al. (1981) and more recently by Deines (2004). According to the calculations, cerussite should be approximately 6‰ (Deines, 2004) to 7‰ (Golyshev et al., 1981) depleted in ^{13}C compared to calcite at a temperature of 27 °C. However, the studies yielded contradictory results for smithsonite. Golyshev et al. (1981) determined a smithsonite–calcite carbon isotope fractionation of approximately +6.2‰ at 27 °C, while the results of Deines (2004) indicate a value of −1.3‰. No experimental results are currently available for Pb and Zn carbonates.

3. Analytical methods

Isotope analyses were performed at Bayerische Staatssammlung für Paläontologie, Munich, Germany. Carbon dioxide was extracted from carbonates by reaction with phosphoric acid at 72 °C using an

automated on-line device (Finnigan Gasbench II). Oxygen and carbon isotope ratios were measured with a Finnigan Deltaplus mass spectrometer operated in a continuous He flow mode. We used the phosphoric acid fractionation factors given in Section 2.1. The isotope results are expressed as delta values in permil (‰) relative to VSMOW for oxygen and VPDB for carbon. The precision and accuracy of the isotope values is estimated at ±0.2‰ (1σ). Samples that come from the South Australian Museum, Department of Mineralogy, are identified by the prefix SAM and the local sample number, while samples from the Mineralogische Staatssammlung München have the prefix MSM in Table 1.

4. Stable isotope geochemistry of supergene deposits

4.1. Iglesiente district, SW Sardinia, Italy

The geology of calamine deposits of SW Sardinia has been recently reviewed by Boni et al. (2003a,b). The nonsulfide deposits formed by paleoweathering of pre-Variscan stratabound Sedex and MVT type deposits hosted by Paleozoic carbonates, as well as minor post-Variscan vein, paleokarst and skarn deposits. The oxidized ores comprise both primary sulfide and carbonate wall rock replacements, as well as open space fillings, speleothems, and transported calamine ore in a hyperkarstic environment. The oxidation zones reach to depths of 200 to more than 600 m below the present surface, and are considered to be fossil oxidation phenomena. The timing of nonsulfide ore formation is not well constrained, but geological and paleomagnetic evidence suggests an Eocene to Plio-Pleistocene age for sulfide oxidation.

Smithsonites from SW Sardinia show a restricted range of δ^{18}O values with an average of 27.4±0.9‰ (1σ, n=26), while carbon isotope values range from −10.4 to −0.6‰ (Boni et al., 2003a). Hydrozincites have isotope compositions within the range of smithsonites. Calcite concretions and crystals associated with smithsonite in calamine ore have consistent oxygen isotope values of 25.1±0.5‰ (n=5) and δ^{13}C values of −11.3 to −9.2‰. Only very few isotope analyses on Pb carbonates (cerussite and phosgenite) were presented by Boni et al. (2003a), and the isotope variability of these minerals was not well constrained. Thus, we have analyzed here a series of cerussites and phosgenites from the Monteponi mine, as well as a cerussite from Tiny–Arenas mine (Table 1, Fig. 2). The Pb carbonates show lower oxygen isotope values and again very little oxygen isotope variability, with average values of 17.4±0.5‰ (n=10) for cerussite and 20.5±0.4‰ (n=6) for phosgenite. In contrast, carbon isotope compositions are again highly variable. The δ^{13}C values of phosgenite (−9.8 to −4.2‰) are within the range of values recorded for smithsonite and calcite, whereas cerussites are characterized by significantly lower carbon isotope values (−21.0 to −6.5‰).

4.2. Liège district, Belgium

The Zn–Pb sulfide ores of Eastern Belgium comprise Mesozoic hydrothermal veins and stratiform replacements of MVT style in Devonian to Carboniferous carbonate rocks (Dejonghe, 1998). These primary sulfide ores have suffered a complex two-stage oxidation history (Coppola et al., 2007-this volume) with a locally important early massive willemite stage of unknown, but possibly low temperature hydrothermal origin, and a late clearly supergene smithsonite–hemimorphite–cerussite stage. The isotope characteristics of smithsonites, cerussites and calcites from the late supergene oxidation zones of La Calamine (Moresnet), Fossey, Theux, Welkenraedt, and Angleur deposits (Coppola et al., 2007-this volume) are almost identical to those of SW Sardinia. Oxygen isotope values of smithsonite (28.4±0.8‰, n=23) are about 10.6‰ heavier than cerussite (17.8±1.0‰, n=5) and 3‰ heavier than calcite (25.4±0.4‰, n=5). The carbon isotope values of smithsonite (−11.6 to −1.8‰) and calcite (−10.4 to −6.1‰) overlap, while those of cerussite are significantly lighter (−18.4 to −14.7‰).

4.3. Broken Hill, New South Wales, Australia

The oxidized zone of the giant metamorphosed Proterozoic Pb–Zn–Ag Broken Hill deposit, New South

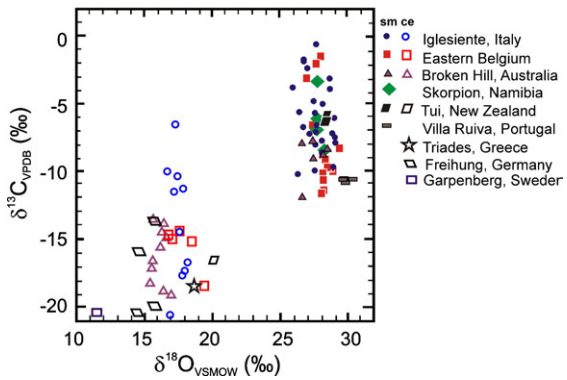

Fig. 2. Carbon and oxygen isotope composition of smithsonites (sm) and cerussites (ce) from supergene oxidation zones of several Pb–Zn deposits (references in the text).

Wales, Australia, extends to about 70 m below the surface, but local oxidation channels reach a depth of 900 m below the surface (Plimer, 1999). The timing of sulfide weathering is not well constrained between Late Cretaceous and Holocene times (Bird and Chivas, 1989, 1993; Alley, 1998; Plimer, 1999). Stable isotope data of cerussite from Block 4, 14 and the Kintore open cuts were presented by Melchiorre et al. (2001). We have recalculated their values (Table 1) using the new phosphoric acid fractionation factors. The oxygen isotope values scatter around 16.2±0.5‰ (n=10), while carbon isotopes range from −19.2 to −13.5‰. An individual carbon isotope value of a cerussite from Broken Hill, NSW, with δ^{13}C of about −12±1‰ was reported by Wickman et al. (1951). Isotope analyses of smithsonite–rhodochrosite solid solutions from the oxidized zone were published by Böttcher et al. (1993). Both oxygen (26.5 to 28.1‰, n=4) and carbon isotope values (−12.6 to −10.0‰) show little variation and no systematic trend with chemical composition. We present here new isotope data on five smithsonite samples from the Broken Hill deposit. The δ^{18}O values range from 26.4 to 28.2‰ and the δ^{13}C values from −8.9 to −7.8‰. There are no published isotope data of unambiguously supergene calcites from the oxidized zone of Broken Hill. Manganoan calcites from fracture and shear zones have oxygen isotope values of 20.5 to 22.9‰ and very low δ^{13}C values of −12 to −47‰ (Böttcher et al., 1993; Gallacher and Plimer, 2000). They are associated with secondary pyrites and are probably related to low-temperature hydrothermal activity (Böttcher et al., 1993). Isotope values of pedogenic calcites from the regional deep regolith, 15 km southeast of Broken Hill, vary from 24.7‰ for oxygen and −8.5‰ for carbon at a depth of 2 m to 29.1‰ for oxygen and 1.8‰ for carbon at 0.75 m (Schmid et al., 2006). This trend is interpreted by Schmid et al. (2006) as a record of paleoclimatic change from cool and humid to hot and arid conditions.

4.4. Other supergene deposits

A much more limited isotope data base (Table 1) exists for supergene Zn, Pb and Ca carbonates in the deposits of Vila Ruiva (Portugal), Skorpion (Namibia), Freihung (Germany), Garpenberg (Sweden), Tui (New Zealand), and Triades (Milos, Greece). The oxygen and carbon isotope data of smithsonites from the Skorpion deposit (Borg et al., 2003) are similar to those from SW Sardinia and E Belgium (Table 1). Smithsonites from the strongly oxidized carbonate-hosted Vila Ruiva deposit in the Ossa-Morena zone, Beija district, SE Portugal, (Carvalhosa, 1965; Vairinho and Fonseca, 1989) show high δ^{18}O values (29.9±0.4‰, n=5), but relatively constant δ^{13}C values (−10.7±0.2‰). A single calcite analysis shows similar oxygen and carbon isotope values. The sandstone-hosted Freihung Pb deposit in NW Bavaria, Germany, (Bjørlykke and Sangster, 1981) is dominated by cerussite formed by oxidation of galena. The oxygen isotope values of cerussite are homogeneous at 15.1±0.4‰ (n=5), while carbon isotope values range from −20.2 to −13.8‰. The lowest oxygen isotope values of cerussite (11.6‰) are reported from the "earthy ores" from the oxidation zone of the Garpenberg Zn–Pb–Cu–Ag deposit, Sweden (Vivallo and Broman, 1993). The δ^{13}C value is −21.2‰. Stable isotope data of smithsonite and cerussite from the oxidation zone of the volcanic-hosted epithermal Tui Pb–Zn–Cu–Ag–Au deposit, New Zealand, were reported by Robinson (1974). Smithsonites are about 8‰ heavier in oxygen values and about 10‰ in carbon as compared to cerussite. A single cerussite isotope analysis was reported by Liakopoulos (1987) from the oxidation zone of the volcanic-hosted Triades Pb–Zn–Ba deposit, Milos island, Greece. The carbon isotope values is low (−18.5‰), but similar to most supergene cerussites, and the oxygen isotope value is 18.7‰ (VSMOW).

4.5. Summary of isotope characteristics of supergene Pb–Zn deposits

The investigated supergene Pb, Zn, and Ca carbonate minerals from supergene oxidation zones of sulfide deposits show a very similar, systematic pattern of oxygen and carbon isotope distribution in the δ–δ plot (Fig. 2). The variation of oxygen isotope compositions is limited within a deposit indicating relatively constant isotope compositions of the oxidation fluid and constant temperatures. This is consistent with observations of ground waters associated with undisturbed oxidizing massive sulfide deposits (Leybourne et al., 2006). The cerussites have δ^{18}O values that are 11±1‰ lower than cogenetic smithsonites and hydrozincites, 7.5±0.5‰ lower than calcites or aragonites, and 3±0.5‰ lower than phosgenites. The range of carbon isotope values (−12 to 0‰) of supergene smithsonites, phosgenites and calcites in many deposits reflects variable contributions from at least two sources of carbon and similar carbon isotope fractionation factor for these minerals. Cerussites from supergene deposits, however, have much lower δ^{13}C values (−21 to −6‰) than supergene smithsonites, phosgenites or calcites from the same deposit.

5. Submarine formation of Pb and Ca carbonates: the Lavrion slag minerals, Greece

Empirical calibrations of isotope fractionation in terrestrial environments using minerals formed in the vadose zone of old mines (e.g., Melchiorre et al., 2001) are hampered by uncertainties in both formation temperature and water isotope composition, as both parameters may show significant seasonal variations especially in continental climates. We, therefore, studied base metal carbonates formed recently in a submarine environment, as variations of water isotope compositions are negligible and temperature variations moderate. The ancient marine slags from the Lavrion area, Greece, contain more than hundred species of secondary minerals crystallized in small cavities (Gelaude et al., 1996). The crystals are generally less than 2 mm in size (Fig. 3) and formed during the last 2500 years by reaction of sea water with Pb-rich glassy material of the slags. The slags were recovered from about 4 to 6 m depth at the Thorikos and Vrissaki area. The temperature of crystallization is constrained between 15 °C in winter and 25 °C in summer and the oxygen isotope composition of the Mediterranean Sea water is +1.5± 0.3‰ (Stahl and Rinow, 1973; Kennedy et al., 2001). The carbon isotope composition of Mediterranean Sea water is variable depending on local photosynthetic activity (e.g., Kennedy et al., 2001). We have analyzed the C and O isotope composition of aragonite, Mg-calcite, cerussite and phosgenite from the slags to better constrain fractionation factors of both lead carbonate minerals (Table 2). Unfortunately, secondary Zn minerals are extremely rare in the slags, as Zn is evaporated during the smelting process. The cerussites have $\delta^{18}O$ values of 24.8±0.2‰ (n=6) and $\delta^{13}C$ values ranging from −5.7 to −3.2‰, while oxygen (27.9±0.8‰, n=6) and carbon isotope values (−3.5 to −0.4‰) of phosgenites are higher (Fig. 4). Aragonites and a single Mg–calcite from the cavities in the slags show $\delta^{18}O$ values of 31.5±1.3‰ (n=8) and variable carbon isotope values (−5.9 to −0.3‰). The isotope compositions of cerussites, phosgenites and calcite from calamine ores in the Iglesiente district, Sardinia, are consistently about 8‰ lower than those of the Lavrion submarine slag minerals (Fig. 4). This provides further evidence that Mediterranean seawater did not play any role in sulfide oxidation and especially phosgenite formation in the

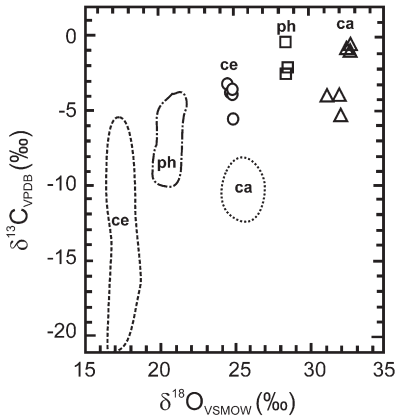

Fig. 4. Stable isotope composition of cerussite (ce), phosgenite (ph) and calcium carbonate minerals (ca) from the Lavrion marine slags (individual symbols) and from the supergene oxidation zones of the Iglesiente mining district, Italy (fields).

Fig. 3. Aragonite (left), cerussite (middle), and phosgenite (right) in cavities formed by submarine alteration of ancient Pb-rich slags from Lavrion, Greece. Width of each picture: 5 mm.

Table 2
C and O isotope data of Pb and Ca carbonates from the ancient marine slags of Lavrion, Greece

Sample No	Mineral	Description	$\delta^{13}C_{VPDB}$	$\delta^{18}O_{VSMOW}$
Lav-2	Cerussite		−5.7	25.0
Lav-5 (29161a)	Cerussite		−4.0	24.7
Lav-5 (29161b)	Cerussite		−3.4	24.9
Lav-3 (29160a)	Cerussite		−3.7	24.8
Lav-3 (29160b)	Cerussite		−3.9	24.6
Lav-14	Cerussite		−3.2	24.5
Lav-1	Phosgenite	Clear prismatic crystal	−3.5	28.1
Lav-4 (29157)	Phosgenite	Clear prismatic crystal	−3.0	28.3
Lav-12	Phosgenite	Clear prismatic crystal	−0.3	28.6
Lav-13	Phosgenite	Clear prismatic crystal	−3.4	26.7
Lav-6a	Aragonite	White crust	−4.1	29.9
Lav-6b	Aragonite	White crust	−5.9	29.4
Lav-7	Aragonite	Clear botryoidal crust	−3.9	32.1
Lav-8	Aragonite	Fine needles	−4.2	31.2
Lav-15a	Aragonite	Fine needles	−0.3	32.8
Lav-15b	Aragonite	Fine needles	−0.9	32.6
Lav-16	Aragonite	Fine needles	−0.3	32.2
Lav-10	Mg-calcite	Botryoidal crust	−5.4	31.8

Iglesiente district (Boni et al., 2003a). The aragonite oxygen isotope data yield formation temperatures of 20±6 °C using a $\delta^{18}O$ value of +1.5‰ for the Mediterranean sea water and the calcite–water fractionation equation of O'Neil et al. (1969). These values are in excellent agreement with the local average surface seawater temperatures. However, it has been suggested that the oxygen isotope fractionation is different for aragonite and calcite (see for example Zhou and Zheng, 2003; Kim et al., 2006, for recent compilations). Application of the oxygen isotope fractionation equation of Zhou and Zheng (2003) yields slightly lower temperatures of 15±5 °C, while the biogenic aragonite–water fractionation equation of Grossman and Ku (1986), that is favored by recent experimental studies (e.g., Kim et al., 2006), gives higher temperatures of 26±6 °C, i.e., close to maximum summer temperatures. Other suggested equations yield values in between the two. The application of the cerussite thermometer of Melchiorre et al. (2001), however, yields unrealistically high temperatures of 37±1 °C.

6. Discussion

6.1. Oxygen isotope fractionation factors in carbonate–water systems

Our empirical well-constrained isotope fractionation data from the Lavrion slags are used in combination with the experimental data of O'Neil et al. (1969) to derive an oxygen isotope fractionation equation between cerussite and water as a function of temperature below 240 °C:

$$1000\ln\alpha_{\text{cerussite–water}} = 2.29(10^6/T^2) - 3.56 \quad (6)$$

Our new equation (Fig. 5) predicts a calcite–cerussite fractionation of 5.8 to 7.2‰ below 40 °C, which is consistent with both theoretical estimates (6.0 to 9.6‰, Golyshev et al., 1981; Zheng, 1999) and our empirical data from the supergene oxidation zones (~7.5±0.5‰). We note, however, that most calcites in calamine ores formed clearly after Pb and Zn carbonates (e.g., Boni et al., 2003a), possibly as a consequence of climatic change toward more arid conditions similar to pedogenic carbonates (Cerling, 1984). Thus, Ca and Pb/Zn carbonates from calamine ores may not necessarily be in isotopic equilibrium. One of the previous empirical

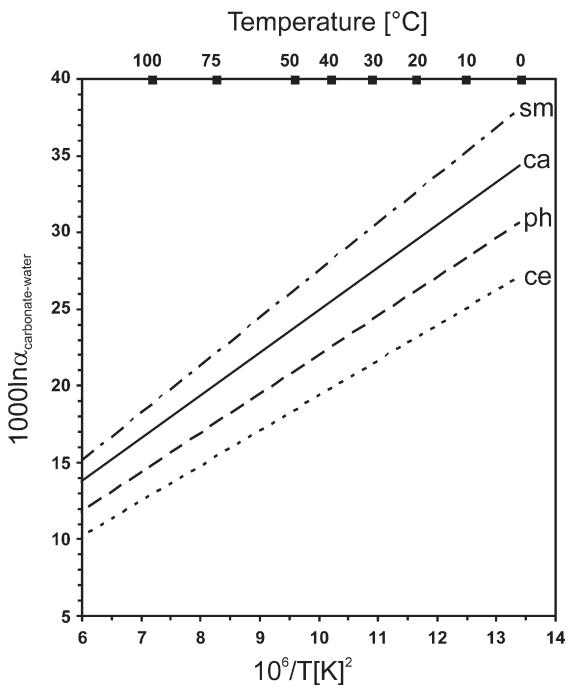

Fig. 5. New oxygen isotope fractionation equations between carbonate minerals and water. Cerussite (ce), phosgenite (ph), calcite (ca) and smithsonite (sm).

cerussite–water fractionation estimates (a cerussite from the Bwlch Glas Mine; Melchiorre et al., 2001) plots very close (within 1‰) to our new equation. However, the second empirical calibration point of Melchiorre et al. (2001) from the Pinnacles Mine, Broken Hill region Australia, is about 3‰ higher than our estimate at the same temperature (23 °C). We consider the estimate in a continental arid region (Pinnacles Mine) using a single isotope measurement of the mine water less reliable than measurements in more humid regions (e.g., Bwlch Glas Mine), as variations of monthly mean oxygen isotope compositions of local meteoric waters in continental arid areas are much larger, e.g., more than 10‰ at Alice Springs, Australia (IAEA, 2004), than in coastal humid areas, e.g., less than 2.5‰ at Valentia, Ireland (IAEA, 2004). The two aforementioned IAEA/WMO stations are located closest to the two mines and have a continuous isotope record of more than 3 years. The experimental calibration of Melchiorre et al. (2001) using a synthesis approach from reaction of Pb-rich solutions with calcite yields much larger cerussite–water fractionations (about 4‰ at 20 °C) than our calibration. Synthesis experiments, however, cannot rigorously demonstrate the attainment of isotopic equilibrium (e.g., Chacko et al., 2001).

The oxygen isotope fractionation equations for smithsonite–water and phosgenite–water are more difficult to establish, as high temperature experiments do not exist for the two minerals. Two aspects have to be considered here. Smithsonites and phosgenites of supergene sulfide oxidation zones are 11 ± 1‰ and 3 ± 0.5‰, respectively, heavier than co-genetic cerussites and the oxygen isotope fractionation between carbonate minerals decreases with increasing temperature (O'Neil et al., 1969; Chacko et al., 2001). The former observation results in decreasing A values in the fractionation equation of the form $1000\ln\alpha_{\text{mineral–water}} = A * 10^6/T^2 + B$ for minerals that have a decreasing tendency to incorporate the heavy isotope, for example the A value is 3.14 for siderite–water (Carothers et al., 1988), 2.78 for calcite–water (O'Neil et al., 1969) and 2.29 for cerussite (this study). Using a constant B value (−3.50) and appropriate A values that predict to our observed fractionations, we suggest the following $^{18}O/^{16}O$ fractionation equations for smithsonite and phosgenite:

$$1000\ln\alpha_{\text{smithsonite–water}} = 3.10(10^6/T^2) - 3.50 \quad (7)$$

$$1000\ln\alpha_{\text{phosgenite–water}} = 2.55(10^6/T^2) - 3.50. \quad (8)$$

Our new equations (Fig. 5) predict the observed fractionations at low temperatures, but are speculative at temperatures above 100 °C. The smithsonite–water fractionation is only slightly (<0.4‰) smaller than the siderite–water fractionation (Carothers et al., 1988). This is consistent with theoretical estimates (Golyshev et al., 1981; Zheng, 1999). Thus, the isotope compositions of the common solid solutions between smithsonite and siderite, e.g., "*monheimite*", can be easily interpreted with our new equation. Our few data on hydrozincites suggest that the oxygen isotope fractionation factors for this mineral and water are similar to those of smithsonite, but further studies are required. The phosgenite–water fractionation is within 0.5‰ of the witherite–water fractionation equation of O'Neil et al. (1969), but clearly distinct from those of cerussite–water.

6.2. Geothermometry and paleoclimatic implications

We have calculated equilibration temperatures for carbonate minerals from supergene sulfide oxidation zones using our new equations and the estimated isotope values of paleometeoric waters. The paleometeoric water compositions are generally based on calculations using stable isotope data of kaolinites found within the deposits (Bird and Chivas, 1989) or in adjacent saprolites (Gilg, 2000; Yans, 2003) and/or isotope data of meteoric carbonate cements in combination with fluid inclusion data (Muchez et al., 1998), or pedogenic carbonates (Schmid et al., 2006). If such data do not exist for a region, e.g., Southern Namibia (Skorpion) or Portugal (Vila Ruiva), we have used available isotope data of groundwaters (Dachroth and Sonntag, 1983) or precipitation (IAEA, 2004). Our results (Table 3) show that all investigated smithsonites, cerussites, phosgenites, and calcites yield temperatures in the range between +8 and +30 °C consistent with a supergene origin. The average values for minerals with more than one analysis cluster even more tightly at 20 ± 6 °C. Variation of isotope composition of the water by 1‰ results in temperatures changes of about 5 °C. The temperatures for various minerals from the same deposit generally yield consistent temperatures. However, this is in part related to the new calibrations of oxygen isotope fraction factors, especially for smithsonite and phosgenite. The formation temperatures for Pb and Zn carbonates from Sardinia (11 to 23 °C) are much lower and in our view more realistic than the previous estimates (20 to 35 °C; Boni et al., 2003a) that were based the fractionation equations of Zheng (1999) and Melchiorre et al. (2001).

Our results, therefore, do not confirm earlier evidence (Melchiorre et al., 1999, 2000, 2001; Melchiorre and Williams, 2001) for unusually high

Table 3
Results of oxygen isotope geothermometry of Pb and Zn carbonate using estimated isotope compositions of local paleometeoric water (PMW)

Location	Mineral	Number of analyses	$\delta^{18}O_{VSMOW}$ (‰) Ave. (Min/Max)	PMW (‰)	Ref.	T (°C) Ave. (Min/Max)
Lavrion (slag)	Cerussite	6	24.8 (24.5/25.0)	1.5	1	20 (19/22)
	Phosgenite	4	27.9 (26.7/28.6)	1.5	1	21 (17/27)
Iglesiente	Smithsonite	14	27.6 (25.7/28.9)	−6.5	2	15 (11/23)
	Cerussite	10	17.4 (16.7/18.0)	−6.5	2	16 (13/20)
	Phosgenite	6	20.7 (20.1/21.2)	−6.5	2	16 (14/19)
Liège	Smithsonite	23	28.4 (27.1/30.2)	−6	3	14 (8/19)
	Cerussite	5	17.8 (16.8/19.3)	−6	3	17 (9/22)
Broken Hill	Smithsonite	6	27.6 (26.4/28.7)	−6	4	17 (11/20)
	Cerussite	5	16.2 (15.4/16.9)	−6	4	26 (30/22)
Skorpion	Smithsonite	5	27.8 (27.5/28.3)	−6	5	17 (15/18)
Vila Ruiva	Smithsonite	5	29.9 (29.6/30.6)	−4.5	6	14 (12/16)
Freihung	Cerussite	6	15.1 (14.5/15.7)	−9	7	15 (12/18)
Garpenberg	Cerussite	1	11.6	−13	8	12
Triades	Cerussite	1	18.7	−6	9	12
Tui	Smithsonite	2	28.1	−6	10	15
	Cerussite	1	19.7	−6	10	7

References: 1 Stahl and Rinow (1973), Kennedy et al. (2001), 2 Boni et al. (2003a,b), De Vivo et al. (1987), 3 Muchez et al. (1998), Yans (2003), 4 Herczeg et al. (2001), Melchiorre et al. (2001), 5 Dachroth and Sonntag (1983), 6 IAEA (2004), 7 Gilg (2000), 8 Moser et al. (1989), 9 Liakopoulos (1987), 10 Robinson (1974).

temperatures in excess of 40 °C in oxidation zones of sulfide-rich deposits. These authors invoke exothermic sulfide oxidation reactions as the heat source. This mechanism, however, may only be applicable when sulfide oxidation and carbonate precipitation occurs in the vadose zone where oxygen is easily available. The low concentration of dissolved oxygen in water and the high heat capacity of water rule out the viability of such oxidative heating processes within the phreatic zone (e.g., Leybourne et al., 2006). Large cerussite crystals in small pockets within massive galena ore in the deepest part of the Monteponi mine (samples SPE-26 and MSM 52511) have the same oxygen isotope composition and thus calculated temperature as the disseminated cerussites crystallized in vuggy goethite-rich gossans (samples SPE-28 and HAM-1).

The isotope data from the Broken Hill deposit may possibly indicate unusual variations of formation temperatures between smithsonites (17 °C) and cerussite (26 °C). Such systematic temperature differences between different cogenetic minerals are in our opinion not very likely, and probably related to the small and not-representative sample number. A very similar temperature range of 15 to 25 °C can be calculated from the O–H isotope compositions of kaolinites from the oxidation zone of the Broken Hill ($\delta^{18}O = 17.1$ to 19.9‰; $\delta D = -75$ to -66‰; $n = 4$; Bird and Chivas, 1989) using the fractionation equations of Sheppard and Gilg (1996) and assuming equilibrium with water isotope compositions on the Global Meteoric Water Line ($\delta D = 8 * \delta^{18}O + 10$). Thus, isotope thermometry of both kaolinites and base metal carbonates indicate formation temperatures of less then 40 °C for the oxidation zone minerals at Broken Hill.

It is remarkable that the average calculated formation temperatures of Pb and Zn carbonates show relatively limited variations around 20 °C while the range of oxygen isotope compositions of the minerals is quite significant; for example, the $\delta^{18}O$ values of cerussites range from 11.6 to 25.0‰. In Fig. 6, we have plotted the $\delta^{18}O$ values of the carbonate minerals against the estimated isotope value of paleometeoric waters. The graph shows a linear relationship for each mineral and most data points are located between the 10 and 20 °C equilibrium isotherm. Modern pedogenic calcites from Africa, North America and Europe (Cerling, 1984) follow a very similar trend along the 10 °C isotherm. Thus, the oxygen isotope compositions of supergene Pb and Zn carbonates and pedogenic carbonates are directly related to that of the meteoric water with some alteration caused by evaporation in the case of pedogenic carbonates (Cerling, 1984; Alonso-Zarza, 2003) and a minor temperature effect. Thus, oxygen isotope data of pedogenic carbonate and supergene Pb and Zn carbonates can be used to estimate oxygen isotope compositions of paleometeoric waters. The latter are related to a variety of climatic factors, among which the mean annual air temperature appears to be the most important (e.g., Fricke and O'Neil, 1999; Dworkin et al., 2005). Thus, oxygen isotope data of supergene base metal carbonates could potentially be used as paleoclimatic indicators, similar to pedogenic carbonates (Dworkin

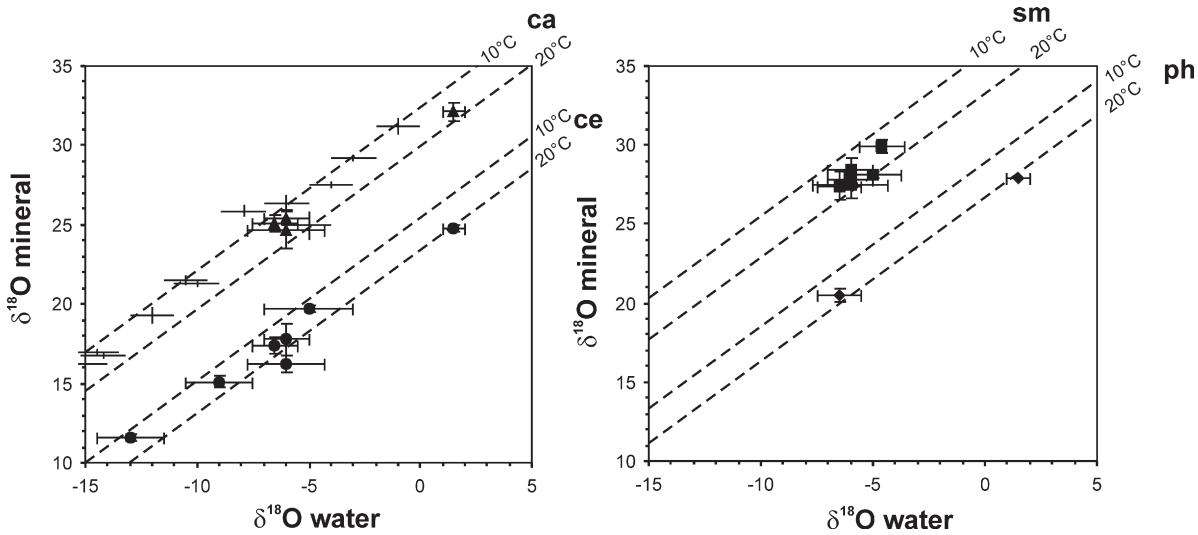

Fig. 6. Oxygen isotope data of cerussite (ce, circles), calcites (ca, triangles), phosgenites (ph, diamonds), and smithsonites (sm, squares) from supergene oxidation zones mentioned in the text, including the Lavrion marine slags and estimated corresponding local paleometeoric water compositions. Black crosses without symbol: modern pedogenic calcites (Cerling, 1984).

et al., 2005), meteoric calcite cements (Hays and Grossman, 1991), or clay minerals (Gilg, 2000), if the base metal carbonate minerals retain their isotope signatures.

6.3. Carbon isotope values of supergene carbonates

The carbon isotope values of smithsonite from the oxidation zone from carbonate-hosted deposits (Iglesiente, Italy; Liège, Belgium) show large variations of 12‰ between 0 and −12‰, while cerussites range from −9 to −21‰ with a single value at −6.5‰. These observations indicate that at least two isotopically distinct sources of carbon were involved in the formation of the secondary base metal carbonates (Boni et al., 2003a) and that the carbon isotope fractionation factors for the two minerals differ significantly. The variation of $\delta^{13}C$ values of smithsonite and cerussite from the silicate-hosted deposits of Broken Hill, Freihung, and Skorpion is less pronounced, smaller than 6.5‰. This could either be related to the predominance of one carbon source or to the generally smaller and thus less representative sample number we have for these deposits. We also note that smithsonites from the carbonate-hosted Vila Ruiva deposit show an extremely small variation of $\delta^{13}C$ values (10.7±0.3‰; $n=5$). Thus, variability of carbon isotope values of secondary base metal carbonates may not necessarily be related to the nature of the host rocks.

The ^{13}C-depleted component in smithsonites with $\delta^{13}C$ values around −12‰ is similar to the isotope composition of pedogenic calcite formed in soils with predominant C3 vegetation (e.g., Cerling, 1984) and thus may be related to soil CO_2. Oxidation of sulfide-oxidizing bacteria within sulfides ores as a consequence of a dropping water table has been suggested as an alternative source for ^{13}C-depleted carbon in supergene carbonates (e.g., Melchiorre et al., 2001; Melchiorre and Enders, 2003). Three possible sources for the ^{13}C-enriched component in smithsonite with $\delta^{13}C$ values around 0‰ can be envisaged: CO_2 from wall rock carbonates, atmospheric CO_2, and soil CO_2 derived from decomposition of C4 plants (Cerling, 1984). We consider the release of CO_2 by reaction of acid fluids created by sulfide oxidation with isotopically heavy sedimentary, diagenetic, or hydrothermal carbonates from the wall rocks as the most probable source of the second carbon component in supergene carbonates. As sedimentary, diagenetic and hydrothermal carbonates may occasionally reach $\delta^{13}C$ values of +5 to +10‰, we can expect such high values also in supergene smithsonites.

Our study on smithsonsites from the Iglesiente district, Sardinia, (Boni et al., 2003a) suggested that botryoidal and stalactitic shaped crystals, that probably formed in the vadose zone, are dominated by the ^{13}C-enriched component, while other types of smithsonites are generally depleted in ^{13}C. Such relationships between morphology and carbon isotope composition were not detected in the calamines of the Liège district, Belgium (Coppola et al., 2007-this volume) and Broken Hill, Australia (this study). Cerussites from SW Sardinia have both high and low carbon isotope values irrespective of

location within the oxidation zone, i.e., in pockets within the massive sulfides from the deepest parts and in cavities of the gossan from the uppermost part.

The calcites associated to smithsonites are dominated by the isotopically light carbon component and have comparable carbon isotopic compositions to smithsonites. Thus, our data suggest that carbon isotope fractionation between calcite and smithsonite at ambient temperatures is small, probably less than ~2‰, consistent with previous suggestions (Melchiorre et al., 2001; Deines, 2004). The carbon isotope values of cerussites are, however, systematically lower by about 9‰ compared to smithsonites and calcites from the same deposit. These empirical data corroborate the previous theoretical estimates of significant carbon isotope fractionation between these carbonates (Golyshev et al., 1981; Deines, 2004). The isotope data from the Lavrion slags, however, do not show these large carbon isotope differences between cerussites and calcium carbonates (calcite and aragonite). This could be related to a very specific environment of carbonate formation in the cavities of the slags ("closed system"). If the crystallization of the carbonate quantitatively precipitates the dissolved carbon in the cavities, then according to the law of mass conservation, the carbonate will inherit the isotope composition of the initially dissolved carbon species, and variable fraction factors between minerals and dissolved species are less important. The situation may be different in oxidized sulfide deposits ("open system") where a continuous supply of new oxidized organic soil or wall rock carbon in the oxidizing fluid established a relatively large dissolved carbon pool and mineral fractionation factors play a more significant role in the isotope compositions of the newly formed carbonates. Individual outliers, such as the cerussite MSM 52514 from the Monteponi mine, Sardinia, with an unusually high $\delta^{13}C$ value of −6.5‰, could be explained by a local closed system behavior during carbonate precipitation in supergene oxidation zones.

7. Conclusions

Oxygen isotope data of Pb and Zn carbonates from supergene sulfide oxidation zones and slag minerals from Lavrion, Greece, formed in the marine environment, have been used to derive new equations of oxygen isotope fractionation for various Pb and Zn carbonate minerals (cerussite, phosgenite, smithsonite, and hydrozincite) and water as a function of temperature. Our new equations for cerussite and smithsonite differ significantly from those previously published (Zheng, 1999; Melchiorre et al., 2001) that were based on synthesis experiments and bond-type modeling.

The isotope compositions of Pb and Zn carbonates from supergene deposits show a characteristic pattern of relatively constant oxygen and often highly variable carbon isotope compositions. Application of our new fractionation equations to natural assemblages from surficial oxidation zones of sulfide deposits yield formation temperatures of about 20±5 °C that are consistent with a supergene origin. No evidence for unusually high temperatures (>40 °C) in sulfide-rich ores has been detected in any of the studied deposits. However, given the uncertainties in the estimate of the isotope compositions of the paleometeoric waters and the mineral–water fractionation factors, the precise determination of terrestrial paleotemperatures using oxygen isotope compositions of supergene Pb and Zn carbonates is problematic. The secondary base metal carbonates studied here principally formed as open space filling. Thus, further studies focusing on possible isotope differences of secondary Pb and Zn carbonates that originate by sulfide or wall-rock carbonate replacement are needed.

Stable oxygen and carbon isotope geochemistry has also great potential in identifying and characterizing hydrothermal Pb and Zn carbonates. Thermodynamic calculations (Brugger et al., 2003) suggest that smithsonite is at least theoretically stable at temperatures of 100 °C and more, if CO_2 fugacities are high and the activity of silica is low. Few possible candidates for hypogene Zn and Pb carbonates have been suggested in the literature. Minčeva-Stefanova (1989) described a rare hydrothermal mineralization phase of mainly dolomite, pink cobaltian smithsonite, sphalerite, barite, and quartz with minor galena, calcite, aragonite, and cobaltian mimetite in veins and cavities of the stratiform Sedmochislenitsi Pb–Zn(–Cu) deposit, Bulgaria. New studies on the Angouran Zn deposit, Iran (Gilg et al., 2003a; Gilg and Boni, 2004; Boni et al., in press) have detected large variations of oxygen isotope values (>4‰) and concomitant little variation of carbon isotope values for early stage smithsonites that are accompanied by unusual pyrite, galena, and arsenopyrite precipitation. Similarly, large oxygen isotope variations characterize smithsonites and cerussites from the very deep oxidation zones of the Tsumeb deposit, Namibia (Gilg et al., 2003c). Microthermometric data on cerussites and wulfenites from this deposit indicate minimum formation temperatures of about 50 °C. Unusually low oxygen isotope values were reported recently on hypogene smithsonite (17.0‰) from the Neves-Corvo VHMS deposit, Portugal, by Relvas et al. (2006) and from a

ferrous smithsonite (20.4‰) from Montevecchio, Sardinia, by Boni et al. (2003a). Other possible hypogene smithsonites were observed in some Upper Silesian Zn–Pb deposits, Poland (Kucha and Czajka, 1984), and the Vazante deposit, Brazil (Monteiro et al., 1999). Further detailed stable isotope studies are necessary to characterize hypogene Pb and Zn carbonates.

Acknowledgements

We like to thank Joel Brugger for supplying smithsonite samples from the Broken Hill deposits (NSW, Australia), Thomas Sperling and Günter Grundmann for additional cerussite samples from Sardinia, and Christian Rewitzer for the photographs. The constructive reviews by Tony Fallick and Jochen Hoefs are greatly appreciated.

References

Alley, N.F., 1998. Cainozoic stratigraphy, paleoenvironments and geological evolution of the Lake Eyre Basin. Palaeogeography, Palaeoclimatology, Palaeoecology 144, 239–263.

Alonso-Zarza, A.M., 2003. Paleoenvironmental significance of palustrine carbonates and calcretes in the geological record. Earth-Science Reviews 60, 261–298.

Bawden, T.M., Einaudi, M.T., Bostick, B.C., Meibom, A., Wooden, J., Norby, J.W., Orobona, M.J.T., Chamberlain, C.P., 2003. Extreme ^{34}S depletions in ZnS at the Mike gold deposit, Carlin Trend, Nevada: evidence for bacteriogenic supergene sphalerite. Geology 31, 913–916.

Bird, M.I., Chivas, A.R., 1989. Stable-isotope geochronology of the Australian regolith. Geochimica et Cosmochimica Acta 53, 3239–3256.

Bird, M.I., Chivas, A.R., 1993. Geomorphic and palaeoclimatic implications of an oxygen-isotope chronology for Australian deeply weathered profiles. Australian Journal of Earth Sciences 40, 345–358.

Bjørlykke, A., Sangster, D.F., 1981. An overview of sandstone lead deposits and their relationship to red-bed copper and carbonate-hosted lead–zinc deposits. Economic Geology 75th Anniversary Volume, pp. 179–213.

Boni, M., Gilg, H.A., Aversa, G., Balassone, G., 2003a. The "Calamine" of SW Sardinia (Italy): geology, mineralogy and stable isotope geochemistry of a supergene Zn-mineralization. Economic Geology 98, 731–748.

Boni, M., Aversa, G., Balassone, G., Gilg, H.A., 2003b. The Zn–Pb ore deposits in SW Sardinia (Italy): from sulfides to "calamine". In: Andrew, C., Ashton, J., Boland, M., Cruise, M., Earls, G., Fusciardi, L., Kelly, J., Stanley, G. (Eds.), The Geology and Genesis of Europe's Major Base Metal Deposits. Irish Association for Economic Geology, pp. 283–291.

Boni, M., Gilg, H.A., Balassone, G., Schneider, J., Allen, C.A., Moore F., in press. Hypogene Zn carbonate ores in the Angouran deposit, NW Iran. Mineralium Deposita. doi:10.1007/s00126-007-0144-4.

Borg, G., Kärner, K., Buxton, M., Armstrong, R., Schalk, W.V.D., 2003. Geology of the Skorpion supergene zinc deposit, southern Namibia. Economic Geology 98, 749–771.

Böttcher, M.E., Gehlken, P.-L., Birch, W.D., Usdowski, E., Hoefs, J., 1993. The rhodochrosite–smithsonite solid-solution series from Broken Hill (NSW), Australia: geochemical and infrared spectroscopic investigations. Neues Jahrbuch für Mineralogie Monatshefte 1993, 352–362.

Brugger, J., McPhail, D.C., Wallace, M., Waters, J., 2003. Formation of willemite in hydrothermal environments. Economic Geology 98, 819–835.

Carothers, W.W., Adami, L.H., Rosenbauer, R.J., 1988. Experimental oxygen isotope fractionation between siderite–water and phosphoric acid liberated CO_2–siderite. Geochimica et Cosmochimica Acta 52, 2445–2450.

Carvalhosa, A.B., 1965. Contribução para o conhecimento geológica da região entra Portel and Ficalho (Alentejo). Serviços Geológicos de Portugal Memória 11, 1–138.

Cerling, T.E., 1984. The stable isotopic composition of modern soil carbonate and its relationship to climate. Earth and Planetary Science Letters 71, 229–240.

Chacko, T., Cole, D.R., Horita, J., 2001. Equilibrium oxygen, hydrogen and carbon isotope fractionation factors applicable to geologic systems. Reviews in Mineralogy and Geochemistry 43, 1–81.

Coppola, V., Boni, M., Gilg, H.A., Balassone, G., Dejonghe, L., 2007-this volume. The "calamine" nonsulfide Zn–Pb deposits of Belgium: petrographical, mineralogical and geochemical characterization. Ore Geology Reviews. doi:10.1016/j.oregeorev.2006.03.005.

Dachroth, W., Sonntag, C., 1983. Grundwasserneubildung und Isotopendatierung in Südwestafrika/ Namibia. Zeitschrift der Deutschen Geologischen Gesellschaft 134, 1013–1041.

Deines, P., 2004. Carbon isotope effects in carbonate systems. Geochimica et Cosmochimica Acta 68, 2659–2679.

Dejonghe, L., 1998. Zinc–lead deposits of Belgium. Ore Geology Reviews 12, 329–354.

De Vivo, B., Maiorani, A., Perna, G., Turi, B., 1987. Fluid inclusion and stable isotope studies on calcite, quartz and barite from karstic caves in the Masua mine, southwestern Sardinia, Italy. Chemie der Erde 46, 259–273.

Dworkin, S.I., Nordt, L., Atchley, S., 2005. Determining terrestrial paleotemperatures using the oxygen isotopic composition of pedogenic carbonate. Earth and Planetary Science Letters 237, 56–68.

Field, C.W., 1966. Sulfur isotopic method for discriminating between sulfates of hypogene and supergene origin. Economic Geology 61, 1428–1435.

Field, C.W., Fifarek, R.H., 1985. Light stable isotope systematics in the epithermal environment. Reviews in Economic Geology 2, 99–128.

Fricke, H.C., O'Neil, J.R., 1999. The correlation between $^{18}O/^{16}O$ ratios of meteoric waters and surface temperature: its use in investigating terrestrial climate change over geological time. Earth and Planetary Science Letters 170, 181–196.

Friedman, I., O'Neil, J.R., 1977. Compilation of stable isotope fractionation factors of geochemical interest. USGS Professional Paper, vol. 440-KK, pp. 1–12.

Gallacher, A., Plimer, I.R., 2000. The origin of fault zone minerals at Broken Hill, New South Wales. Journal and Proceedings of the Royal Society of New South Wales 133, 14–15.

Gavelin, S., Parwel, A., Ryhage, R., 1960. Sulfur isotope fractionation in sulfide mineralization. Economic Geology 55, 510–530.

Gelaude, P., van Kalmthout, P., Rewitzer, C., 1996. Lavrion, the minerals in the ancient slags. Janssen Print, Nijmegen. 194 pp.

Gilg, H.A., 2000. D–H evidence for the timing of kaolinization in Northeast Bavaria, Germany. Chemical Geology 170, 5–18.

Gilg, H.A., Boni, M., 2004. Stable isotope studies on Zn and Pb carbonates: their role in mineral exploration of non-sulphide deposits. Proceedings, SEG Conference, Perth WA, September 2004, pp. 361–365.

Gilg, H.A., Allen, C., Balassone, G., Boni, M., Moore, F., 2003a. The 3-stage evolution of the Angouran Zn "oxide"–sulfide deposit, Iran. In: Eliopoulos, D.G., et al. (Ed.), Mineral Exploration and Sustainable Development. Millpress, Rotterdam, pp. 77–80.

Gilg, H.A., Struck, U., Vennemann, T., Boni, M., 2003b. Phosphoric acid fractionation for smithsonite and cerussite between 25 and 72 °C. Geochimica et Cosmochimica Acta 67, 4049–4055.

Gilg, H.A., Hochleitner, R., Keller, P., Struck, U., 2003c. A fluid inclusion and stable isotope study of secondary oxidation minerals from the Tsumeb Cu–Pb–Zn deposit, Namibia. Proceedings ECROFI XI, Budapest, Hungary, June 5–7, 2003. Acta Mineralogica-Petrographica (Szeged), Abstract Series, vol. 2, pp. 78–79.

Golyshev, S.I., Padalko, N.L., Pechekin, S.A., 1981. Fractionation of stable oxygen and carbon isotopes in carbonate systems. Geokhimiya 10, 1427–1441.

Grossman, E.L., Ku, T.L., 1986. Oxygen and carbon isotope fractionation in biogenic aragonite: temperature effects. Chemical Geology (Isotope Geoscience Section) 59, 59–74.

Hays, P.D., Grossman, E.L., 1991. Oxygen isotopes in meteoric calcite cements as indicators of continental plaeoclimate. Geology 19, 441–444.

Herczeg, A.L., Dogramaci, S.S., Leaney, F.W., 2001. Origin of dissolved salts in a large, semi-arid groundwater system: Murray Basin, Australia. Marine and Freshwater Resources 52, 41–52.

Hitzman, M.W., Reynolds, N.A., Sangster, D.F., Allen, C.R., Carman, C., 2003. Classification, genesis, and exploration guides for non-sulfide zinc deposits. Economic Geology 98, 685–714.

IAEA, 2004. Isotope Hydrology Information System. The ISOHIS Database. Accessible at: http://isohis.iaea.org.

Kennedy, H., Richardson, C.A., Duarte, C.M., Kennedy, D.P., 2001. Oxygen and carbon stable isotope profiles of the fan mussel, *Pinna nobilis*, and reconstruction of sea surface temperatures in the Mediterranean. Marine Biology 139, 1115–1124.

Kim, S.-T., O'Neil, J.R., 1997. Equilibrium and non-equilibrium oxygen isotope effects in synthetic carbonates. Geochimica et Cosmochimica Acta 61, 3461–3475.

Kim, S.-T., Hillaire-Marcel, C., Mucci, A., 2006. Mechanisms of equilibrium and kinetic oxygen isotope effects in synthetic aragonite at 25 °C. Geochimica et Cosmochimica Acta 70, 5790–5801.

Kucha, H., Czajka, K., 1984. Sulphide–carbonate relationships in the Upper Silesian Zn–Pb deposits (Mississippi Valley-type), Poland, and their genesis. Transactions, Institution of Mining and Metallurgy (Section B, Applied Earth Sciences) 93, 12–22.

Leybourne, M.I., Clark, I.D., Goodfellow, W.D., 2006. Stable isotope geochemistry of ground and surface waters associated with undisturbed massive sulfide deposits; constraints on origin of waters and water-rock reactions. Chemical Geology 231, 300–325.

Liakopoulos, A., 1987. Hydrothermalisme et mineralisations métallifères de l'île de Milos (Cyclades, Grece). Memoires des Sciences de la Terre, Academie de Paris, Université Pierre et Marie Curie, vol. 87–36.

Maréchal, C.N., Télouk, P., Albarède, F., 1999. Precise analysis of copper and zinc isotopic compositions by plasma-source mass spectrometry. Chemical Geology 156, 251–273.

McCrea, J.M., 1950. On the isotope chemistry of carbonates and a paleotemperature scale. Journal of Chemical Physics 18, 849–857.

Melchiorre, E.B., Enders, M.S., 2003. Stable isotope geochemistry of copper carbonates at the Northwest Extension deposit, Morenci district, Arizona: implications for conditions of supergene oxidation and related mineralization. Economic Geology 98, 607–621.

Melchiorre, E.B., Williams, P.A., 2001. Stable isotope characterization of the thermal profile and subsurface biological activity during oxidation of the Great Australia deposit, Cloncurry, Queensland, Australia. Economic Geology 96, 1685–1693.

Melchiorre, E.B., Criss, R.E., Rose, T.P., 1999. Oxygen and carbon isotope study of natural and synthetic malachite. Economic Geology 94, 245–260.

Melchiorre, E.B., Criss, R.E., Rose, T.P., 2000. Oxygen and carbon isotope study of natural and synthetic azurite. Economic Geology 95, 621–628.

Melchiorre, E.B., Williams, P.A., Bevins, R.E., 2001. A low temperature oxygen isotope thermometer for cerussite, with application at Broken Hill, New South Wales, Australia. Geochimica et Cosmochimica Acta 65, 2527–2533.

Minčeva-Stefanova, J., 1989. New facts concerning the formation of hydrothermal sphalerite–smithsonite parageneses. Comptes Rendus de l'Académie Bulgare des Sciences 42, 93–96.

Monteiro, L.V.S, Bettencourt, J.S., Spiro, B., Graça, R., de Oliveira, T.L., 1999. The Vazante zinc mine, Minas Gerais, Brazil: Constraints on willemitic mineralization and fluid evolution. Exploration Mining Geology 8, 21–42.

Moser, H., Wolfa, M., Fritz, P., Fontes, J.-Ch., Florkowski, T., Payne, B.R., 1989. Deuterium, oxygen-18, and tritium in Stripa groundwater. Geochimica et Cosmochimica Acta 53, 1757–1763.

Muchez, P., Nielsen, P., Sintubin, M., Lagrou, D., 1998. Conditions of meteoric calcite formation along a Variscan fault and their possible relation to climatic evolution during the Jurassic–Cretaceous. Sedimentology 45, 845–854.

Ohmoto, H., Rye, R.O., 1979. Isotopes of sulfur and carbon, In: Barnes, H.L. (Ed.), Geochemistry of Hydrothermal Ore Deposits, 2nd edition. Wiley, New York, pp. 509–567.

O'Neil, J.R., 1986. Theoretical and experimental aspects of isotopic fractionation. In: Valley, J.W., Taylor Jr., H.P., O'Neil, J.R. (Eds.), Stable isotopes in high temperature geological processes. Reviews in Mineralogy, vol. 16, pp. 1–40.

O'Neil, J.R., Clayton, R.N., Mayeda, T., 1969. Oxygen isotope fractionation in divalent metal carbonates. Journal of Chemical Physics 51, 5547–5558.

Plimer, I., 1999. The orebodies: the oxidized zone. In: Birch, W.D. (Ed.), Minerals of Broken Hill. Broken Hill City Council, Broken Hill, New South Wales, Australia, pp. 80–87.

Relvas, J.M.R.S., Barriga, F.J.A.S., Longstaffe, F.J., 2006. Hydrothermal alteration and mineralization in the Neves-Corvo volcanic-hosted massive sulfide deposit, Portugal. II. Oxygen, hydrogen, and carbon isotopes. Economic Geology 101, 791–804.

Robinson, B.W., 1974. The origin of mineralization at the Tui mine, Te Aroha, New Zealand, in the light of stable isotope studies. Economic Geology 69, 910–925.

Schmid, S., Worden, R.H., Fisher, Q.J., 2006. Variations of stable isotopes with depth in regolith calcite cements in the Broken Hill region, Australia: Paleoclimatic evolution signal? Journal of Geochemical Exploration 89, 355–358.

Schwinn, G., Wagner, T., Baatartsogt, B., Markl, G., 2006. Quantification of mixing processes in hydrothermal systems by combination of stable isotope and fluid inclusion analyses. Geochimica et Cosmochimica Acta 70, 965–982.

Seal, R.R., 2003. Stable-isotope geochemistry of mine waters and related solids. In: Jambor, J.L., Blowes, D.W., Ritchie, A.I.M. (Eds.), Environmental aspects of mine wastes. Mineralogical Association of Canada Short Course, vol. 31, pp. 303–334.

Sheppard, S.M.F., Gilg, H.A., 1996. Stable isotope geochemistry of clay minerals. Clay Minerals 31, 1–24.

Stahl, W., Rinow, U., 1973. Sauerstoffisotopenanalysen an Mittelmeerwässern. Ein Beitrag zur Problematik von Paläotemperaturbestimmungen. "Meteor" Forschungs-Ergebnisse, Berlin-Stuttgart, Reihe C 14, 55–59.

Vairinho, M.M., Fonseca, E.C., 1989. Distribução do Fe, Mn, Zn, Pb e Cu na zona de oxidação supergénica do jazigo Preguiça (Alto Alentejo, Portugal). Determinação das fases-su-porte do Zn, Pb e Cu por extracção química selectiva sequêncial. Revista da Universidade de Aveiro, Geociências 4, 97–110.

Vivallo, W., Broman, C., 1993. Genesis of the earthy ores at Garpenberg, south central Sweden. Geologiska Föreningens i Stockholm förhandlingar 115, 209–214.

Wickman, F.E., Blix, R., von Ubisch, H., 1951. On the variations in the relative abundances of the carbon isotopes in carbonate minerals. Journal of Geology 59, 142–150.

Yans, J., 2003. Chronologie des sédiments kaoliniques à faciès wealdien (Barrémien moyen et Albien supérieur; Bassin de Mons) et de la saprolite polyphasée (Crétacé inférieur et Miocène inférieur) de la Haute-Lesse (Belgique). Implications géodynamiques et paléoclimatiques. Doctoral Thesis, Faculté Polytechnique de Mons, Belgium, 316 pp.

Zheng, Y.F., 1999. Oxygen isotope fractionation in carbonate and sulfate minerals. Geochemical Journal 33, 109–126.

Zheng, Y.F., Hoefs, J., 1993. Carbon and oxygen isotopic covariations in hydrothermal calcites. Mineralium Deposita 28, 79–89.

Zhou, G.T., Zheng, Y.F., 2003. An experimental study of oxygen isotope fractionation between inorganically precipitated aragonite and water at low temperatures. Geochimica et Cosmochimica Acta 67, 387–399.